

Calculating Auroral Oval Pattern by AE Index*

CHEN Anqin[†](陈安芹), LI Jiawei(李嘉巍), YANG Guanglin(杨光林), and WANG Jingsong(王劲松)

National Center for Space Weather, China Meteorological Administration, Beijing 100081

(Received September 6, 2007; revised January 7, 2008)

ABSTRACT

The relationship between the auroral oval pattern, i.e., location, size, shape, and intensity, and the auroral electrojet activity index (AE index) is studied. It is found that the maximal auroral intensity is elliptically distributed, and the lengths of semimajor and semiminor axes are positively correlated to AE. The intensity along the normal of the auroral oval can be satisfyingly described by a Gaussian distribution, and the maximum and the full width at half maximum of the Gaussian distribution are both positively correlated to AE. Based on these statistical results, a series of experimental formulas as a function of AE are developed to calculate the location, size, shape, and intensity of the auroral oval. These formulas are validated by the auroral images released by SWPC/NOAA.

Key words: auroral oval, AE index (auroral electrojet activity index), linear correlation.

1. Introduction

The auroral electrojet activity index (AE index) is an important parameter indicating the activity of the magnetosphere, which was originally introduced by Davis and Sugiura (1966). Index AE can be obtained from the data of 12 geomagnetic stations located around the auroral oval, the AU and AL indices are the upper and lower envelopes of the horizontal component of geomagnetic field observed by these stations, and express the intensity of the eastward and westward auroral electrojet, respectively. Thus expression $-(AL - AU)$ is defined as AE index, representing the overall intensity of the auroral electrojet (Tu, 1988).

The auroral activity is the most important and intuitional space weather phenomenon in the polar region. Statistical results show that the auroral arc tends to distribute along an oval around geomagnetic latitude 60° (auroral oval) (Feldstein, 1963). The size of the auroral oval varies with the geomagnetic activity, reaching the minimum during the geomagnetic quiet period and expanding to lower latitudes as the geomagnetic field is active (Tu, 1988). The energetic particles in the ring current and radiation belt interact with the waves when a series of intense disturbances were brought about by the solar eruption, and deposite

into the terrestrial upper atmosphere and cause aurora. The deposited particles impact the neutral particles and affect the physical and chemical processes in the mid-upper atmosphere. Meanwhile, H^+ and O^+ upwell into the magnetosphere from the ionosphere and the thermosphere and enhance the ring current (Hao et al., 2006). The spacial scale of the auroral oval is too large to be completely described by the ground-based observations, inspite of the great amount of those observations. It can be done only by the satellites, primarily the polar orbiting ones (Imhof, 1995; Torr, 1995). Unfortunately, the duration of the polar orbiting satellites passing over the polar region is limited, and as a consequence, there is no satellite by far observing the whole auroral oval continuously. This will be improved enormously by the coming KuaFu project, which will carry out continuous imaging of the whole northern auroral oval (Tu et al., 2008). Space Weather Prediction Center (SWPC) of National Oceanic and Atmospheric Administration (NOAA) has developed a technique that uses the power flux observed by a single pass of the NOAA Polar-orbiting Operational Environmental Satellite (POES) over a polar region to construct statistical patterns of auroral power flux, and releases on the website daily <<http://www.swpc.noaa.gov/pmap/index.html>>.

There is an essential connection between AE and

*Supported by the Polar Research Institute of China (KP2005011) and the NSFC under Grant Nos. 40674077 and 40436015.

[†]Corresponding author: chenanqin@cma.gov.cn.

the auroral activity, since AE indicates the geomagnetic variations induced by the auroral electrojet in the polar region. Zhao and Tu (2005) studied the auroral images obtained by Satellite POLAR, and found a positive correlation between the aurora X-ray total intensity and AE. Ostgaard et al. (2002) derived the total energy dissipation (U_A) in the Northern Hemisphere by electron deposition in the energy range from 100 eV to 100 keV, obtained by the observations of Satellite POLAR, and found that there is a linear relation between U_A and $AE^{1/2}$. The relationship between U_A and AE was also studied by Spiro et al. (1982). Assuming some characteristic energy of the deposited electrons and the characteristic width of the auroral oval, some other studies obtained a linear relation between U_A and AE from semiempirical approaches (Perault and Akasofu, 1978; Akasofu, 1981).

These studies suggest a possibility to describe and calculate the characteristics of the auroral oval by AE. In this paper, the relationship between the auroral oval pattern and AE is studied, and a method is developed to calculate the location, size, shape, and intensity of the auroral oval by AE.

2. Data analysis

Aurora is produced by the collisions between the energetic protons and electrons depositing along the magnetic field lines and the molecules and atoms in the upper atmosphere. The POES satellite can monitor the power flux carried by the energetic particles in the energy range of 0.5–20 keV that produce aurora in the atmosphere. Statistical study over 100000 satellite passes comprised the POES historical database, and SWPC has developed a technique to estimate the total deposited power by using observed power flux during a single pass of the satellite over the polar region. The power is sorted into ten auroral activity levels and each level corresponds to a statistical pattern. Based on these patterns, the whole auroral oval can be derived by a single pass observation of POES.

The data set used in this paper contains 340 auroral images of the Northern Hemisphere around 0000 UT relayed by SWPC in 2006. Index AE is obtained

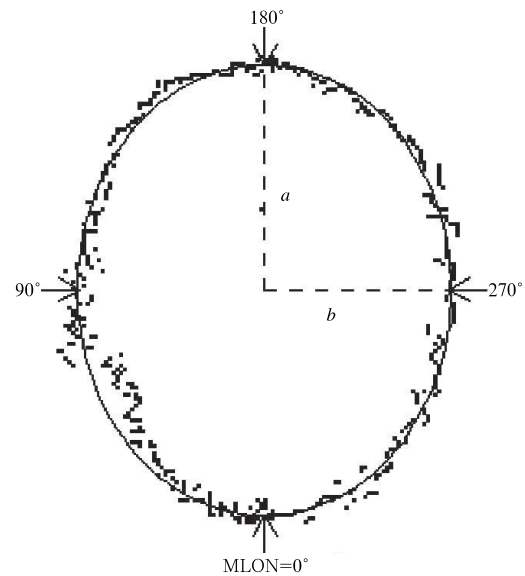


Fig.1. Location of the maximal auroral intensity. The dots are the original data, the solid ellipse is the best fit, $a(b)$ is the semimajor (semiminor) axis of the ellipse, and MLON is the geomagnetic longitude.

from the World Data Center for Geomagnetism, Kyoto <<http://swdcwww.kugi.kyoto-u.ac.jp/aedir>>.

It is found that the maximal auroral intensity is elliptically distributed, and the elliptical center is located near the northern geomagnetic pole (Fig.1), which is consistent with the previous studies and observations (Feldstein, 1963; Akasofu, 1976). However, the location and size of the auroral arc between magnetic longitudes about 30° – 80° depart from the average state obviously. The ellipse can be expressed as

$$\frac{x^2}{a^2} + \frac{y^2}{b^2} = 1, \quad (1)$$

where a (b) is the length of the semimajor (semiminor) axis; x and y are the Cartesian coordinates with the origin at the northern geomagnetic pole.

Figure 2 shows the scattered diagram of the lengths of the semimajor axis (a) and the semiminor axis (b) versus AE for the 340 images. The left panel shows the relationship between a and AE , and it can be seen that there is a linear relation between a and the logarithm of AE ($\ln(AE)$), expressed as

$$a(\text{km}) = 1589.9 + 128.9\ln(AE), \quad (2a)$$

the correlation coefficient (r) and the mean of the absolute deviation (σ) are 0.67 and 118.3, respectively. The right panel shows a similar relationship between b and AE ,

$$b(\text{km}) = 1269.3 + 101.4\ln(AE), \quad (2b)$$

where r equals 0.66 and σ equals 98.6. Most data points are within $\pm 2\sigma$ of the best linear fit for both a and b , and the average relative error is only about 5%.

The results show that the auroral oval changes its size linearly with $\ln(AE)$, and this is actually a quantitative description of the fact that the auroral oval expands to lower latitudes during the geomagnetic activity. Therefore, the semimajor axis a and the semiminor axis b can be obtained by Eq.(2), using the observation or prediction of AE .

Based on the analysis of a large amount of samples, it is found that the intensity along the auroral oval normal can be described by a Gaussian distribution, i.e.,

$$I = I_0 + I_1 e^{-\frac{z^2}{2}}, \quad z = \frac{2\sqrt{2\ln 2}(\varphi - \varphi_0)}{\delta}, \quad (3)$$

where I_0 is the background intensity for various causes (for example, noises), I_1 is the maximal auroral intensity excluding the background intensity, φ is the point

on the normal of the auroral oval, while $\varphi=0$ refers to the crossover point of the normal and the semimajor axis, φ_0 is the location of the auroral intensity maximum, and σ is the full width at half maximum of the Gaussian distribution.

For each auroral oval, some normals are selected to analyze the auroral intensity distributions. The selection of the normals can be arbitrary, and has no essential influence on the result. Without loss of generality, we set geomagnetic longitude 0° shown in Fig.1 as the starting position and select a normal for every 15° . For each normal, fit the intensity with Eq.(3), and one example is shown in Fig.3. It can be seen that the intensity along the auroral oval normal seems to be a Gaussian distribution as shown by dashed lines in Fig.3. All other samples give similar results. Whereas, the intensity between geomagnetic longitudes 30° and 80° is weaker than others, and its statistic characters depart from the average state obviously as well as the location and size.

The relationships between AE and the parameters of the Gaussian distribution along the same normal for all the samples are investigated (Fig.4). It can be seen that I_0 remains nearly constant and changes little with AE , and its mean is $0.017 \text{ erg cm}^{-2} \text{ s}^{-1}$. Figure 4 shows that both I_1 and δ are linearly correlated

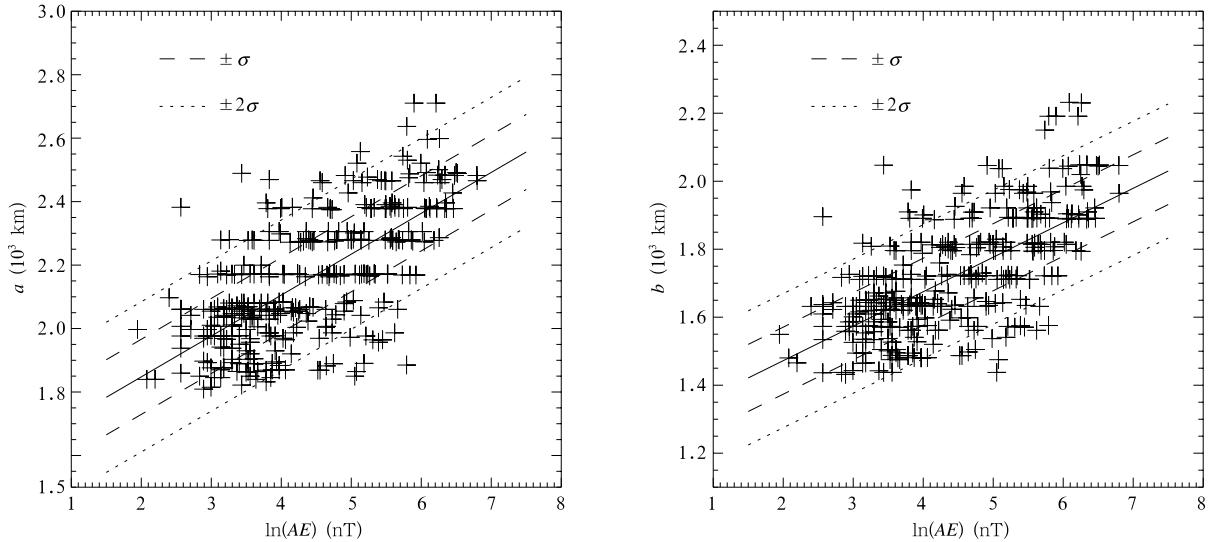


Fig.2. The relationship between the semimajor (semiminor) axis and AE . '+'s are the original data, the solid line is the best linear fit to data points, σ denotes the mean of the absolute deviation, the dashed lines represent the range of $\pm\sigma$, and the dotted line are the range of $\pm 2\sigma$.

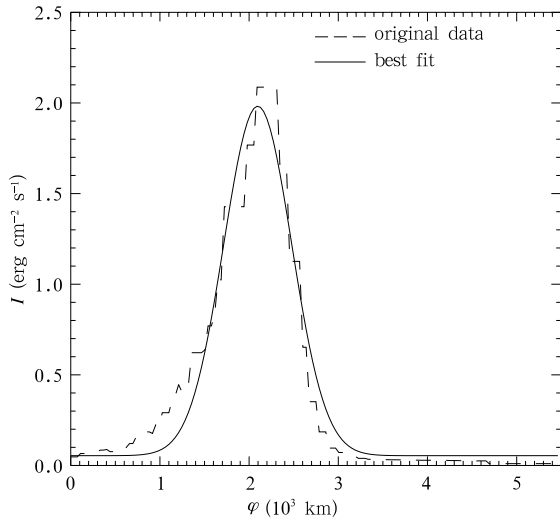


Fig.3. The Gaussian fit of the intensity along the normal of the auroral oval.

to $\ln(AE)$,

$$I_1 (\text{erg cm}^{-2} \text{ s}^{-1}) = -2.81 + 1.04 \ln(AE), \quad (4a)$$

where r equals 0.63 and σ equals 0.94, and

$$\delta (\text{km}) = 181.2 + 100.4 \ln(AE), \quad (4b)$$

where r and σ are 0.65 and 90.6, respectively. Most data points are within the $\pm 2\sigma$ range beside the best linear fit for both I_1 and δ .

Studies on the other normals show the similar results. Therefore, it can be concluded that for all analyzed auroral ovals, the background intensity for the Gaussian distribution along a normal changes little with AE , while the maximum and the full width at half maximum are linearly correlated to $\ln(AE)$, respectively.

The correlation coefficients are not the same for different normals. It is possible to obtain the correlation coefficients for all normals according to the results from all the 24 normals. Assuming that

$$\begin{cases} I_1 (\text{erg cm}^{-2} \text{ s}^{-1}) = A_0 + B_0 \ln(AE) \\ \delta (\text{km}) = A_1 + B_1 \ln(AE), \end{cases} \quad (5)$$

and considering the periodicity along the geomagnetic longitude, we can express all the related parameters as a function of geomagnetic longitude

$$f(x) = C_0 + C_1 \times \sin(x + C_2) + C_3 \times \sin(x + C_4)^2 + C_5 \times \sin(x + C_6)^3, \quad (6)$$

where $f(x)$ represents I_0 , A_0 , B_0 , A_1 , or B_1 , and x is the geomagnetic longitude. Figure 5 shows that Eq.(6) is quite a good description for all the considered parameters.

So far the pattern of an auroral oval can be

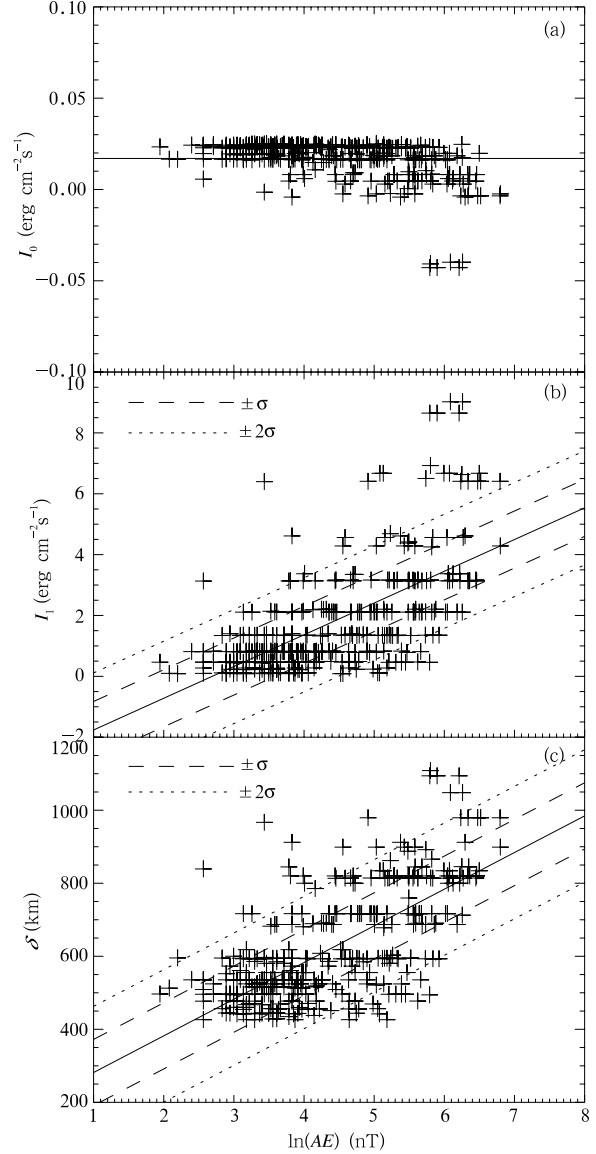


Fig.4. The relationship between AE and the background intensity I_0 (a), the maximal intensity I_1 (b), and the full width at half maximum of the Gaussian fit δ (c). '+'s are the original data and the solid line is the best linear fit, the dashed lines represent the range of $\pm\sigma$, and the dotted lines represent the range of $\pm 2\sigma$.

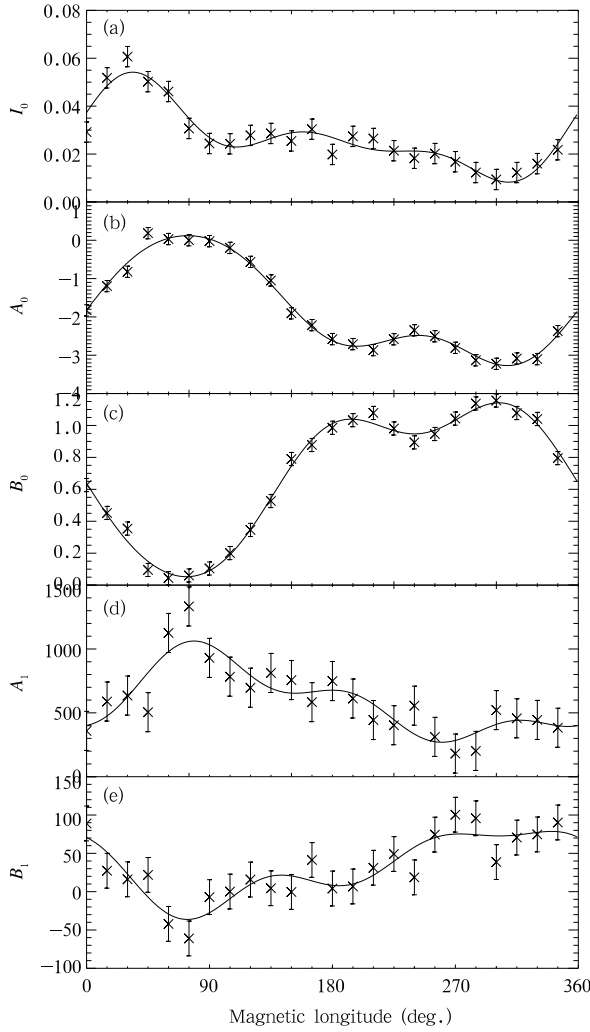


Fig.5. The distributions of I_0 , A_0 , B_0 , A_1 , and B_1 along the maximal intensity ellipse. ‘×’s correspond to the results from Eq.(4), the vertical bar on the cross is the error bar, and the curve is best fit according to Eq.(6).

derived by given AE .

(1) The aurora intensity maximum is located on an ellipse originated at the geomagnetic pole and described by Eq.(2);

(2) The intensity along the oval normal referred to the position of the intensity maximum is described by Eqs.(3) and (5).

Figure 6 shows the comparison of the auroral images released by SWPC and calculated by AE at 0012 UT 10 October 2005. It can be seen that the shape and intensity of the auroral oval are very similar in the two images. It indicates that the method in this

paper is quite acceptable for calculating the shape and intensity of the aurora.

To verify the validity of the method, additional 191 auroral images at about 0000 UT from May to December in 2005 are analyzed. Figure 7 shows the statistical result of the correlation between the auroral images released by SWPC and calculated by AE. It can be seen that for about 60% of the samples their correlation coefficients are greater than 0.9, and for nearly 90% of the samples their correlation coefficients are greater than 0.7. This indicates that our method can satisfyingly reproduce the pattern of auroral ovals released by SWPC. Therefore, this method can be used to calculate the location, size, shape, and intensity of the auroral oval.

3. Conclusions and discussions

Presently, there are a great deal of auroral observations obtained by both ground-based stations and polar satellites. As the auroral oval is too large, the ground-based observation cannot cover the whole auroral oval completely. Meanwhile, the duration of the polar satellite passing polar region is scattered, therefore there is no single satellite can monitor the whole aurora continuously until now.

Considering the essential relationship between AE and the auroral activity, a method is developed to calculate the location, size, shape, and intensity of the auroral oval by AE in this paper. The auroral images released by SWPC are studied, and it is found that the lengths of the semimajor axis and the semiminor axis are both positively correlated to AE , which is a quantitative description of the fact that the auroral oval expands to lower latitudes during the geomagnetic activity. The intensity along the normal of the auroral oval is in Gaussian distribution, the intensity maximum and the full width at half maximum of the Gaussian distribution are also positively correlated to AE , respectively, and the background intensity (e. g., noises) is a roughly constant. Based on these results, a series of experimental formulas as a function of AE are developed to calculate the pattern of the auroral oval. Results show that the location, size, shape, and intensity of the auroral oval calculated by AE is very

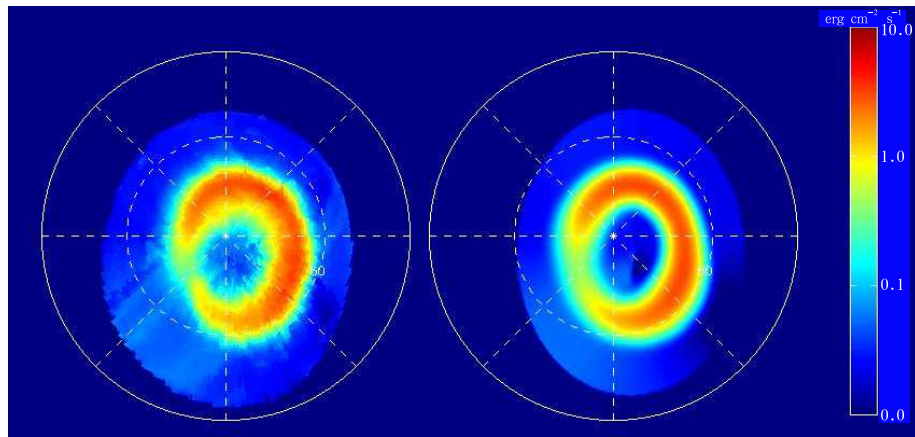


Fig. 6. Comparison of the auroral images released by SWPC (left) and calculated by AE (right).

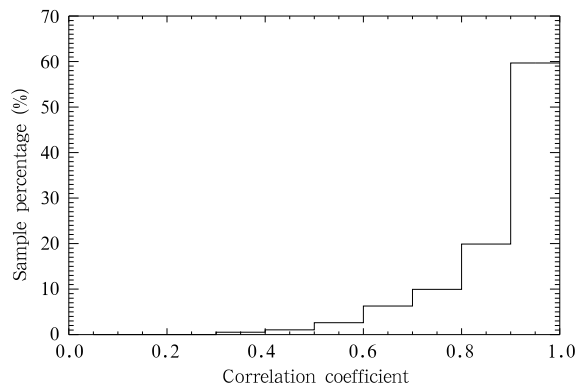


Fig. 7. The correlation between the auroral images released by SWPC and calculated by AE.

similar to the parameters released by SWPC, and 90% of the correlation coefficients between the calculated and SWPC imaged auroral ovals are greater than 0.7.

These results also indicate that our method can be used to predict the auroral oval pattern if AE is predicted.

Many things can be considered to improve our method, e.g., the time identity of the samples, the projective effect, and the variety of the sampling time. Otherwise, for the extremely weak or strong auroral intensity (e.g., the auroral arc between magnetic longitudes 30° and 80°), the result does not match the sample very well. To investigate more data and especially the extreme cases is one possibility for further study.

REFERENCES

- Akasofu, S. -I., 1976: Recent progress in studies of DMSP auroral photographs. *Space Sci. Rev.*, **19**, 169–215.
- Akasofu, S. -I., 1981: Energy coupling between the solar wind and the magnetosphere. *Space Sci. Rev.*, **28**, 121–190.
- Davis, T. N., and M. Sugiura, 1966: Auroral electrojet activity index AE and its universal time variations. *J. Geophys. Res.*, **75**(3), 785–801.
- Feldstein, Y. I., 1963: Some problems concerning the morphology of auroras and magnetic disturbances at high latitudes. *Geomagn. Aeron.*, **3**, 183–192.
- Imhof, W. L., 1995: The polar ionospheric X-ray imaging experiment (PIXIE). *Space Sci. Rev.*, **71**, 385–408.
- Hao Y. Q., Xiao Z., Zou H., and Zhang D. H., 2006: Energetic particle radiations measured by particle detector onboard CBERS-1 satellite. *Chinese Science Bulletin*, **52**(5), 665–670.
- Ostgaard, N., R. R. Nondrak, J. W. Gjerloev, and G. Germany, 2002: A relation between the energy deposition by electron precipitation and geomagnetic indices during substorms. *J. Geophys. Res.*, **107**, 1246–1252.
- Perrault, P., and S. -I. Akasofu, 1978: A study of magnetic storms. *Geophys. J. R. Astron. Soc.*, **54**, 547–573.
- Spiro, R. W., P. H. Reiff, and L. J. Mather Jr, 1982: Precipitating electron energy flux and auroral zone conductances: An empirical model. *J. Geophys. Res.*, **87**, 8215–8227.
- Torr, M. R., D. G. Torr, M. Zukic, et al., 1995: A far ultraviolet imager for the international solar-terrestrial physics mission. *Space Sci. Rev.*, **71**, 329–381.
- Tu C. Y., 1988: *Solar-Territorial Physics*. Science Press, Beijing, 819 pp. (in Chinese)
- Tu C. Y., et al., 2008: Space weather explorer: The KuaFu mission. *Adv. Space Sci.*, **41**, 190–209.
- Zhao L., and Tu C. Y., 2005: A relation between the auroral X-ray total intensity and the substorms index–AE. *J. Geophys.*, **48**(4), 739–743. (in Chinese)